Climatic Change (2009) 95:195–217
DOI 10.1007/s10584-008-9528-4

Effects of climate warming on Olive and olive fly (*Bactrocera oleae* (Gmelin)) in California and Italy

Andrew Paul Gutierrez · Luigi Ponti · Q. A. Cossu

Received: 25 March 2008 / Accepted: 22 September 2008 / Published online: 14 January 2009

Abstract Climate change is expected to alter the geographic distribution and abundance of many species. Here we examine the potential effects of climate warming on olive (*Olea europaea*) and olive fly (*Bactrocera oleae*) across the ecological zones of Arizona–California (AZ–CA) and Italy. A weather-driven physiologically-based demographic model was developed from the extensive literature and used to simulate the phenology, growth and population dynamics of both species. Observed weather for several years from 151 sites in AZ–CA and 84 sites in Italy were used in the study. Three climate-warming scenarios were developed by increasing observed average daily temperature 1°, 2° and 3°C. Predictions of bloom dates, yield, total fly pupae and percent infestation were mapped using GRASS GIS. Linear multiple-regression was used to estimate the effects of weather on yield and fly abundance. Olive has a much wider temperature range of favorability than olive fly. The model predicted the present distributions of both species and gave important insights on the potential effects of climate warming on them. In AZ–CA, climate warming is expected to

A. P. Gutierrez · L. Ponti
Division of Ecosystem Science, ESPM, University of California, Berkeley, CA 94720, USA

A. P. Gutierrez · L. Ponti
Center for the Analysis of Sustainable Agricultural Systems (CASAS), Kensington, CA 94707, USA

L. Ponti
ENEA, Dipartimento BAS, Gruppo "Lotta alla Desertificazione", S.P. Anguillarese 301, 00123 S. Maria di Galeria (Roma), Italy

Q. A. Cossu
Servizio Agrometeorologico Regionale per la Sardegna, Viale Porto Torres 119, 07100 Sassari, Italy

A. P. Gutierrez (✉)
Department of Environmental Science, Policy & Management, University of California, 137 Mulford Hall, Berkeley, CA 94720-3114, USA
e-mail: carpediem@nature.berkeley.edu

contract the range of olive in southern desert areas, and expand it northward and along coastal areas. Olive fly is currently limited by high temperature in the southern part of its range and by cold weather in northern areas. Climate warming is expected to increase the range of olive fly northward and in coastal areas, but decrease it in southern areas. In Italy, the range of olive is expected to increase into currently unfavorable cold areas in higher elevations in the Apennine Mountains in central Italy, and in the Po Valley in the north. Climate warming is expected to increase the range of olive fly northward throughout most of Italy.

1 Introduction

Plants and animals have evolved abiotic requirements and limits for growth, survival and reproduction that with the interactions with other species determine their geographic distribution and abundance (e.g. Andrewartha and Birch 1954). Climate change (Saier 2007) is expected to alter these relationships, but historically it has proven difficult to separate abiotic and biotic effects. Here, we use a physiologically-based weather-driven demographic model (PBDM) to examine the effects of observed weather and three climate warming scenarios on the distribution and abundance of olive (*Olea europaea* L.) and olive fly (*Bactrocera oleae* (Gmelin)) in Arizona–California and Italy. The model simulates the age–mass structured population dynamics of nine functional populations ($n = 1 \ldots 9$): the dynamics of olive leaf mass and numbers {sub models $n = 1, 2$}, stem plus shoots {$n = 3$}, root {4} and fruit mass and number {5, 6}, olive fly in fruit {7}, and reproductive and dormant adults {8, 9}. The biology of the olive system is described below, the details of the model are reviewed in general form in Appendix 1 (see Gutierrez 1996) and the parameters and initial conditions are given in Appendix 2.

1.1 Biology of olive and olive fly

1.1.1 Olive

Olive is a drought tolerant, long-lived species that exhibits little response to photoperiod, and its distribution is limited largely by low and high temperatures, and less so by soil water and other factors (Bongi 2002; Vitagliano and Sebastiani 2002; Fiorino 2003). Temperature affects many aspects of olive's biology: the rates of development (Fig. 1a), photosynthesis, respiration (i.e. the Q_{10} rule), and subunit production rates (leaves, stem, root) initiation (Fig. 1b), and mortality (Fig. 1c). All plant subunits are assumed to have the same thermal thresholds of 9.1°C. The scalar function $\phi_0(T)$ (Fig. 1b) may be viewed as the normalized net of the photosynthetic and respiration rates that define the optimum and the upper and lower thermal thresholds for development. Freezing temperature causes mortality ($\mu_0(T)$) to plant subunits and in the extreme may kill the whole plant (Fig. 1c; see Denney et al. 1985).

The maximum number of flower buds in the current season is a function of the amount of fruit wood produced the previous season, but some of them may be killed by freezing temperatures (Fig. 1c). Approximately 450 h $<$ 7.3°C are required to stimulate spring fruit bud initiation leading to flowering (Hartmann and Opitz 1980; Mancuso et al. 2002; Orlandi et al. 2002; De Melo-Abreu et al. 2004). Approximately 400 degree-days (dd $>$ 9.1°C) are required from bud swelling to flowering

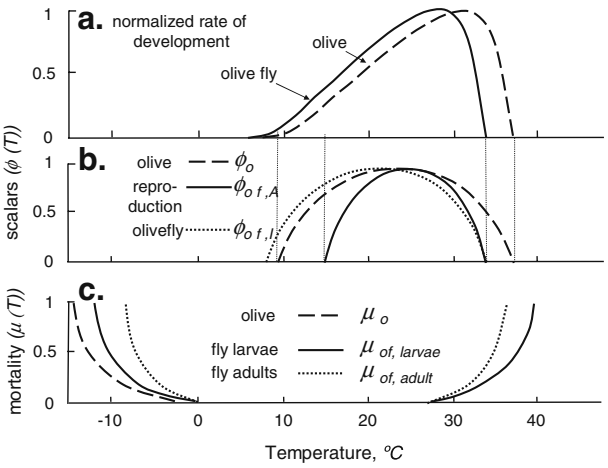

Fig. 1 Effects of temperature on olive and olive fly: **a** normalized developmental rates, **b** temperature scalars ($\phi(T)$) affecting olive and olives fly growth and reproduction, and **c** temperature dependent mortality rates ($\mu(T)d^{-1}$)

(Sanz-Cortés et al. 2002) with the period of flowering being approximately 7–10 days. Massive shedding of young post flower fruit occurs due to lack of pollination, cold weather (Fig. 1c, $\mu_0(T)$; Proietti et al. 1994; Palese et al. 2000), and photosynthate supply shortfalls. A mean of 1495 *dd* are required from flowering to fruit maturation with the fruit becoming susceptible to olive fly when the seed begins to harden.

1.1.2 Olive fly

Olive fly is endemic across the olive growing regions of the Mediterranean Basin and the Middle East. It was first discovered in the Los Angeles basin of California in 1998, and is now widely distributed in the state. The biology of the fly is closely linked to olive fruit age and availability.

Adult flies over-winter in a facultative reproductive-dormancy (Tzanakakis and Koveos 1986; Koveos and Tzanakakis 1990) that begins to break when fruit of increasing age become available (Fletcher and Kapatos 1983), and especially after the seed begins to harden (Fletcher et al. 1978; Girolami 1979; Ricci and Ambrosi 1981). Dormancy may also be induced during summer when fruits are in short supply (Delrio and Prota 1988), when mean temperatures fall below 15°C (Koveos 2001), and during periods of high summer temperatures (Bigler and Delucchi 1981a, b; Crovetti et al. 1981; Bigler 1982; Crovetti et al. 1982). Olive fly females prefer to lay single eggs in unattacked fruit, but multiple attacks may occur when fruit are limiting. Dehisced fruit on the ground play an important role in the fly's dynamics as immature stages in them continue development during the winter (Kapatos and Fletcher 1984).

The effect of temperature on olive fly developmental rate is shown in Fig. 1a, while the effect on reproduction is captured by the scalar function $\phi_{OF}(T)$(____, Fig. 1b; see Appendix 1). The temperature thresholds for olive fly were computed from the literature: 6.3°C for egg–larval stages and 8°C for pupae and adults (Girolami 1979; Crovetti et al. 1982). Mortality of immature stages and adults is also affected by temperature ($\mu_{OF}(T)$, Fig. 1c; Zangheri et al. 1976; Girolami 1979; Crovetti et al. 1981, 1982; Pucci et al. 1981; Kapatos and Fletcher 1986; Delrio and Prota 1988;

Zambetaki et al. 2000; Koveos 2001). In addition, we were aware of a recent laboratory study on survival and development of immature stages on artificial diet (Genç and Nation 2008). The displacement of the larval mortality function in Fig. 1c to lower temperatures corrects for the insulating effects of the fruit on fly immature stages. Depending on temperature, several summer generations may develop (Zangheri et al. 1976) with four to five or more generations occurring in highly favorable areas (Delrio and Prota 1988; Rice et al. 2003).

2 Methods

2.1 Simulation

The model computes many aspects of the daily age structured dynamics of olive and olive fly, but only Julian bloom dates, season yield, cumulative season long olive fly pupae, and the percent of fruit attacked are used as metrics of performance. Runs of the model were for olive alone and with the fly in the absence of pest control. Olive is drought tolerant and hence soil moisture is assumed non-limiting. A batch file was used to run the model across years and locations using site-specific weather data. The geo-referenced data were written by year to an output file for mapping using GIS. The same initial conditions for olive and olive fly were used at all locations, and the model was run continuously for the full simulation period. The model was allowed to equilibrate from the initial conditions during the first year, but the output data were not used to compute means, standard deviations and coefficients of variation.

2.2 Weather data

Site specific daily weather (i.e. daily max–min temperature, solar radiation, rainfall, RH and runs of wind) were used to drive the model. Weather data from 151 locations in AZ–CA for the period 1 January 1995 to 31 October 2006 (http://www.ipm.ucdavis.edu/) and 84 locations in Italy for the period 1 January 1999 to 31 December 2005 (http://www.ucea.it/) were used in the analysis (Fig. 2). Missing data for AZ–CA were estimated by linear interpolation from close temporal data from the same location. Missing Italian data were estimated using inverse distance weighting interpolation of data from the surrounding locations (Mita and Mitasova 2002). Three climate-warming scenarios were created by increasing daily mean temperature 1°, 2° or 3°C assuming all other weather variables remained unchanged.

2.3 GIS mapping and marginal analysis

The GIS software *GRASS*[1] was used to map the data at locations below 700 m. The digital elevation model used is the NOAA Global Land One-km Base Elevation (GLOBE; *www.ngdc.noaa.gov/mgg/topo/globe.html*). USA state boundaries and hydrography data are from the National Atlas of the United States

[1]Software initially developed by the US Army Corp of Engineers and currently maintained and developed by the Geographic Resources Analysis Support System (GRASS) Software, ITC-irst, Trento, Italy (http://grass.itc.it).

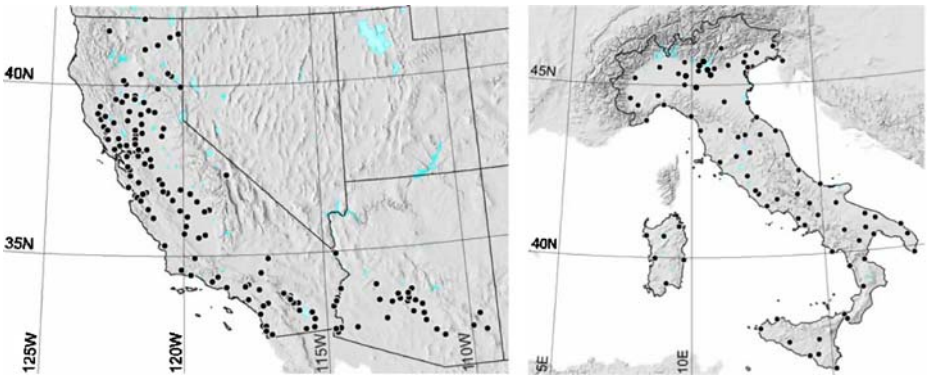

Fig. 2 Weather stations in Arizona–California and Italy used in the simulation study

(*www.nationalatlas.gov/atlasftp.html*). Boundaries and hydrography data from the National Geospatial Agency (Vector Map Level 0, *earth-info.nga.mil/publications/vmap0.html*) were used for Italy. All GIS datasets used are available in the public domain. Inverse distance weighting interpolation was used to map the simulation data, and hence the patterns reflect not only the site specific effects of weather on the biology of the species but also the location and distances between weather stations.

For heuristic purposes, the simulation data across years and locations were analyzed using linear multivariate regression retaining only independent variables having slopes significantly greater than zero (t-values, $p < 0.05$).

3 Results

3.1 Phenology of olive and olive fly at Davis, CA

Simulation results for the year 2000 at Davis in Central California were taken from a longer run to illustrate some of the richness of the model. The patterns each year depends on the previous year's fruit wood production, flowering date, fruit retention, adult fly survival and density as initial conditions, and the year's weather.

The left-hand scale in Fig. 3a depicts the numbers of fruit bud initiated and the pattern of retention of maturing fruit, while the right scale shows the percentage of fruit attacked. Note that a sharp drop in fruit numbers occurs shortly after flowering.

Dormant fly adults surviving from the previous year (Fig. 3b) begin to attack olive fruit on roughly Julian day 150 (Fig. 3c) with the percentage of fruit attacked reaching ca. 80% by day 270 (Fig. 3a). The within season dynamics of olive fly immature stages suggest four summer generations with a partial one occurring after harvest in shed or unpicked fruit. A 95% harvesting efficiency is assumed in the model. Reproductive dormancy is induced in adult flies during periods of high temperatures (after day 250) and after harvest at Davis, but the patterns will vary considerably across years and locations.

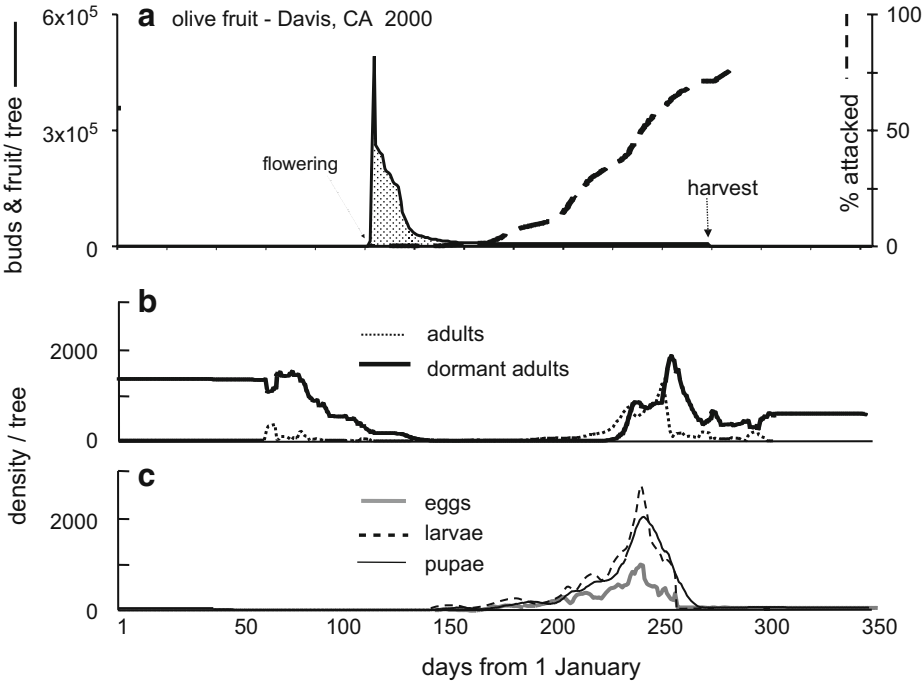

Fig. 3 Simulated phenology for olive and olive fly at Davis, CA during 2000: **a** olive flowering, retention and percent fruit attacked, **b** reproductively dormant and non dormant adults and **c** olive fly eggs, larvae and pupae

3.2 Regional dynamics and the effects of climate change

The dynamics of olive and olive fly are known to vary widely across the ecological zones of AZ–CA and Italy, and these will change with climate warming. Mean bloom dates, yield, total pupae over the season and the percent attacked fruit under observation and three climate warming scenarios are compared.

3.2.1 Physiological time

For ease of comparison, season length in AZ–CA and Italy is summarized in degree-days for olive (dda > 9.1°C; Fig. 4a, c). The ranges of dda in AZ–CA (1434–2980 dda) are similar to those in Italy (1,512–2,690 dda) despite very different topographies, distance to ocean and latitude. The ranges of standard deviations (*STD*) are also similar (Fig. 4b vs. d).

3.2.2 Bloom dates

Sufficient chilling for flower bud initiation accrued at all locations and years in AZ–CA resulting in a range of mean bloom dates using historical weather of Julian days 80–163 with blooming occurring earliest in hotter areas of southern California and Arizona (Fig. 5a, see histograms). Blooming occurs later in Italy where the range of bloom dates is 114–178 (Fig. 5e).

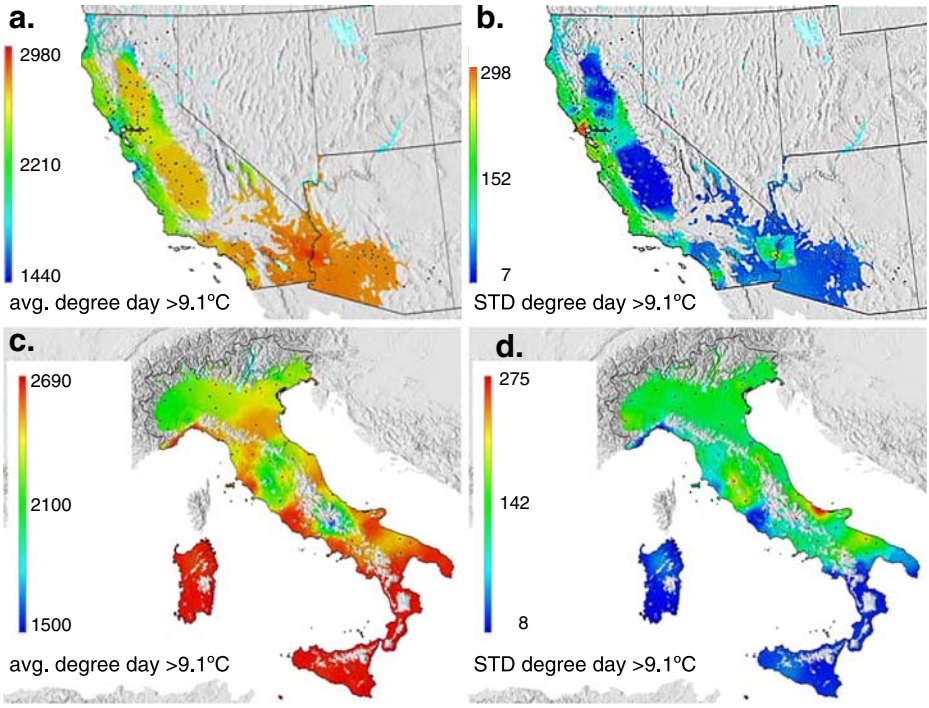

Fig. 4 Average degree-days >9.1°C (**a**, **c**) and standard deviation (*STD*; **b**, **d**) for Arizona–California and Italy respectively

In AZ–CA, a dramatic shift toward earlier blooming occurs throughout much of north and central California with increasing temperatures (histograms for Fig. 5b–d). Specifically, a three-day decrease in bloom dates occurs per 1°C rise in mean temperature at the lower end of the range, while the effect on the upper end is less clear.

In Italy, the lower and upper end of the range of blooming dates decreases 6–8 days per 1°C increase in mean temperature. The effects of warming are not readily discernible in the GIS maps (Fig. 5f–h) but are easily seen as shifts in the histograms.

3.2.3 Yield w/o olive fly

In AZ–CA, mean yields (kg fruit dry matter/ tree) using observed weather and in the absence of olive fly are predicted to be highest in the warmer southern areas (Fig. 6a). Olive is not heavily planted there due to alternative higher value crops and legislation on allergenic pollen (ag.arizona.edu/pima/gardening/aridplants/Olea_europaea.html). Lowest yields are predicted along the cool coast of northern California. Coefficients of variation of yield in AZ–CA were generally small (<10–15%, not shown). With +1°C in temperature, yields increased everywhere, especially in the southern half of the Great Central Valley and along the coast of Southern California (Fig. 6b). However, with a +2°C increase, yields increase further along the

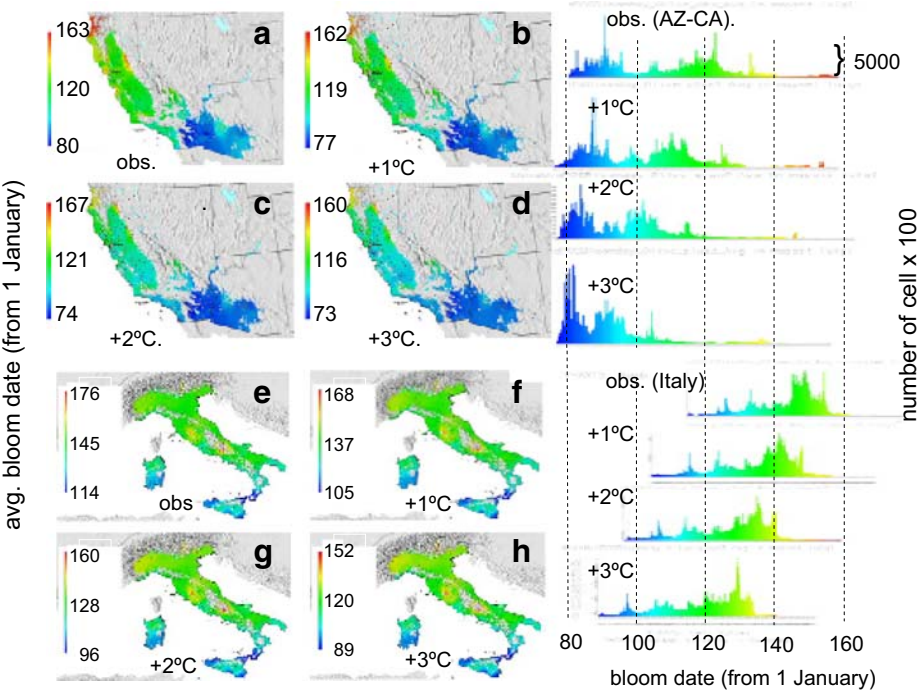

Fig. 5 Average bloom date in AZ–CA (**a**–**d**) and Italy (**e**–**g**) under observed (*obs*) weather and three climate-warming scenarios (+1, +2 and +3°C). The histograms at the right are the distributions of cell ×100 in each bloom date class with a reference value of 50 × 100 indicated in top histogram

coast and in central California (Fig. 6c). With +3°C, decreases in yield are predicted in the southern central valley and in the inland regions of southern California and Arizona but yield is predicted to increase in northern areas and along the coast (Fig. 6d). Decreases in yield in hotter regions with increased warming are due to increased respiration costs.

In Italy, highest yields using observed weather are predicted in southern regions (e.g. Puglia, Calabria), and Sicily and Sardinia islands with very low yields predicted at higher elevations in Central Italy (i.e. the Apennines) and in the colder areas of the Po Valley south of the Alps (Fig. 6e). The Po Valley and the Apennines are not centers of olive culture and the predicted coefficients of variation are >50% (not shown). The model captures olive production around Garda Lake in Northern Italy (see inset for Fig. 6e) where a favorable microclimate is created by the lake. Favorable areas around Lago Trasimeno in the Apennines near Perugia in Central Italy were missed due to lack of available weather data. Increasing temperatures 1° to 3°C cause yields to increase everywhere with the largest increases predicted in northern currently unfavorable areas (Fig. 6e vs. f–h).

Regression analysis—the effects of season length (dda > 9.1°C), total ddb<0°C, date of bloom (Blm) and cumulative yearly rainfall (mm) on yield (g dry matter) across all ecological zones and climate change scenarios were captured using linear multiple regressions (Eqs. 1i, 1ii for AZ–CA and Italy respectively). No obvious biological interactions were apparent among the variables, hence none were included

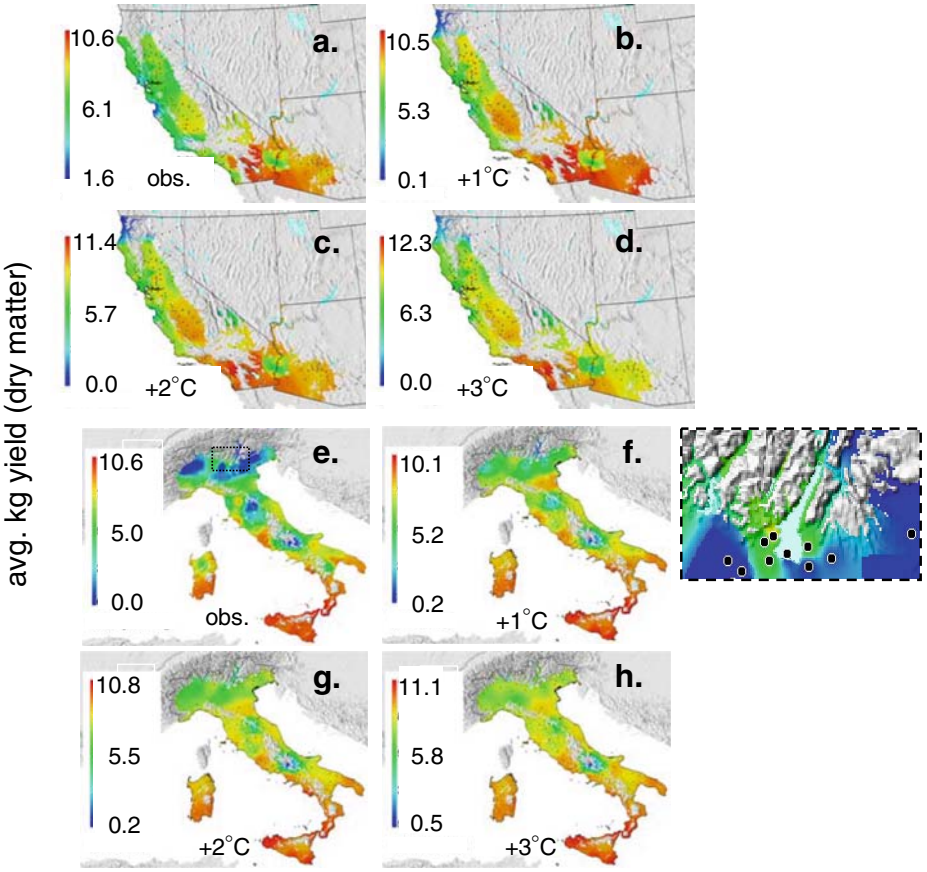

Fig. 6 Average yield (kg tree^{-1}) in Arizona–California (**a**–**d**) and Italy (**e**–**h**) under observed weather and three climate-warming scenarios (+1, +2 and +3°C). The *inset* from **e** illustrates microclimate effects on yield around Garda Lake

in the regression analysis. The means for the independent variable are given to allow estimation of the mean effects.

For AZ–CA, all independent variables are highly significant ($p < 0.01$) with dda having a positive effect, and ddb, Blm and mm having negative effects (Eq. 1i). Substituting mean values for the independent variables shows that dda contributes 5699.7 g to yield with bloom date (−1325.3), ddb (−1034), and mm (−168.3) having negative effects.

$$\text{yield}_{\text{AZ-CA}} = 4301.5 + 2.153\text{dda} - 5.50\text{ddb} - 12.612\text{Blm} - 0.396\text{mm}$$
$$df = 6, 567,\ R^2 = 0.59,\ F = 2, 360.0 \qquad \text{(1i)}$$
$$(\text{AZ} - \text{CA means: dda} = 2651;\ \text{ddb} = 188.0;\ \text{Blm} = 105.1,\ \text{mm} = 425.1)$$

A mean of 7,166.3 + 2971.0 g tree^{-1} is predicted across all sites in AZ–CA.

For Italy, date of bloom is not significant while the regression coefficient for dda is positive and those for ddb and mm are negative.

$$\begin{gathered}\text{yield}_{\text{Italy}} = 5,043.6 + 1.93\text{dda} - 7.26\text{ddb} - 1.18\text{mm} \\ df = 2,096,\ R^2 = 0.37,\ F = 402.0 \\ (\text{Italy means: dda} = 2,588;\ \text{ddb} = 303.0;\ \text{mm} = 793)\end{gathered} \tag{1ii}$$

Substituting the mean values for independent variables shows that dda contribute 4994.8 g while ddb and mm decrease yield by −2199.8 g and −935.7 g respectively. A mean of 6,656.0 + 4,051.6 g of olive tree^{-1} is predicted across all sites in Italy.

3.2.4 Olive fly

Total season-long number of pupae produced is used as a metric of the fly's invasive potential given the bottom-up effects of olive fruit abundance and phenology, and temperature. The areas predicted to be most favorable for olive fly in AZ–CA are along the southern coast where temperatures remain mild throughout the year (Fig. 7a), while the desert regions of AZ–CA are generally unfavorable due to high summer temperatures that increase fly mortality and decrease reproduction directly and cause reproductive dormancy. The high summer temperature in the Great Central Valley allow only low to intermediate densities of the fly to develop. Climate warming is expected to cause the favorable range for olive fly to contract further in the Central Valley and desert regions of AZ–CA, but to increase it in coastal areas (Fig. 7b–d).

In Italy, only the northern regions and the mountains of central Italy are unfavorable due to winter temperatures, but as with yield, the area around the larger lakes (e.g. Garda Lake) were favorable for olive fly because winter temperatures are moderated by the water (inset in Fig. 7e). With climate warming, areas favorable for olive fly move increasingly northward into previously inhospitable cold areas of the Po Valley but decease in the more southern areas due to increased summer temperature (Fig. 7f–h).

Regression analysis—the coefficients of the linear multiple regression model (AZ–CA, Eq. 2ii of $\log_{10}$ pupae on total ddb < 0°C, date of bloom (Blm) and cumulative year long rainfall (mm) were highly significant ($p < 0.01$), while the significance level for dda was $p < 0.05$. Only the coefficients for dda and ddb were negative.

$$\begin{gathered}\text{Log}_{10}\text{pupae}_{\text{AZ–CA}} = 5.151 - 0.000646\text{dda} - 0.00187\text{ddb} \\ +0.0018\text{Blm} + 0.00039\text{mm} \\ df = 6,567,\ R^2 = 0.44,\ F = 1288.4 \\ (\text{AZ–CA means: dda} = 2,612;\ \text{ddb} = 231.4.0;\ \text{Blm} = 104.8,\ \text{mm} = 418.9)\end{gathered} \tag{2i}$$

Substituting mean values for the independent variables shows that dda (i.e. $-0.000646 \times 2612 = -1.688$) followed by ddb (−0.433) have the greatest mean negative impact on log pupal density, while Blm (0.189) and mm (0.163) have positive effects resulting a mean of 2,421.0 pupae per tree across AZ–CA.

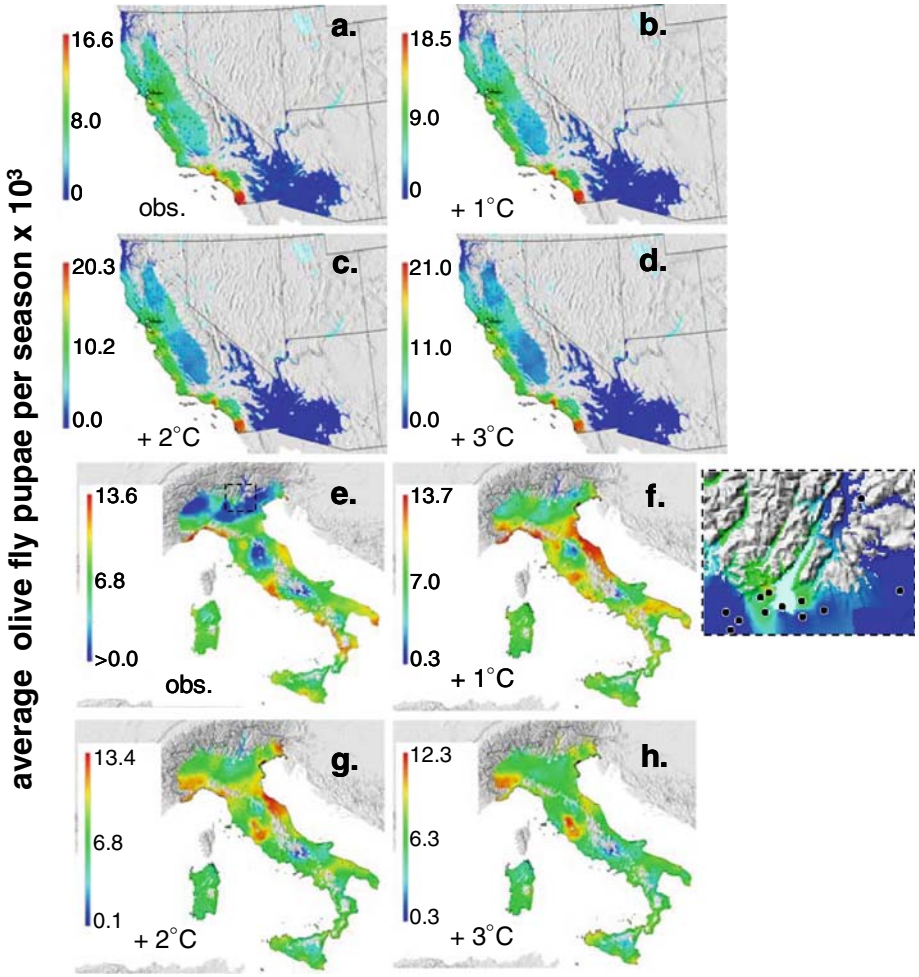

Fig. 7 Average cumulative olive fly pupae (10^3 tree^{-1}) per season in Arizona–California (**a**–**d**) and Italy (**e**–**h**) under observed weather and three climate-warming scenarios (+1, +2 and +3°C). The *inset* from **e** illustrates microclimate effects around Garda Lake

For Italy (2ii), all regression coefficients were highly significant with only those for ddb and mm being negative.

$$\begin{aligned} \mathrm{Log}_{10}\mathrm{pupae}_{\mathrm{Italy}} &= -2.988 + 0.0018\mathrm{dda} - 0.0022\mathrm{ddb} \\ &\quad + 0.020\mathrm{Blm} - 0.0003\mathrm{mm} \\ df = 2095,\ R^2 &= 0.44,\ F = 414.3 \\ (\text{Italy means: dda} &= 2583;\ \mathrm{ddb} = 306.2;\ \mathrm{Blm} = 130.1;\ \mathrm{mm} = 794.3) \end{aligned} \tag{2ii}$$

Using mean values for the independent variables shows that dda has the greatest positive influence on log pupal density (4.857), followed by Blm (2.537) with ddb and mm having negative impact (−0.679 and −0.238 respectively) yielding an mean of

3,085.7 pupae per tree. The lower mean density of pupae in AZ–CA relative to Italy (2,421.0 vs. 3,085.7) is due to the large number of sites in unfavorable areas included in the regression model.

3.2.5 Percentage of fruit attacked

Results for percentage of fruit attacked should be interpreted with caution as the values are dimensionless and do not reflect either fruit or fly density.

For California, the percentage of fruit attacked using observed weather makes intuitive sense as very low rates are predicted in areas unfavorable for olive fly (see Fig. 7a) and are high in areas of known olive culture. Many inland areas of current high risk (yellow–red, Fig. 8a) are predicted to have decreased risk with climate warming due to the negative effects of increasing summer temperatures on

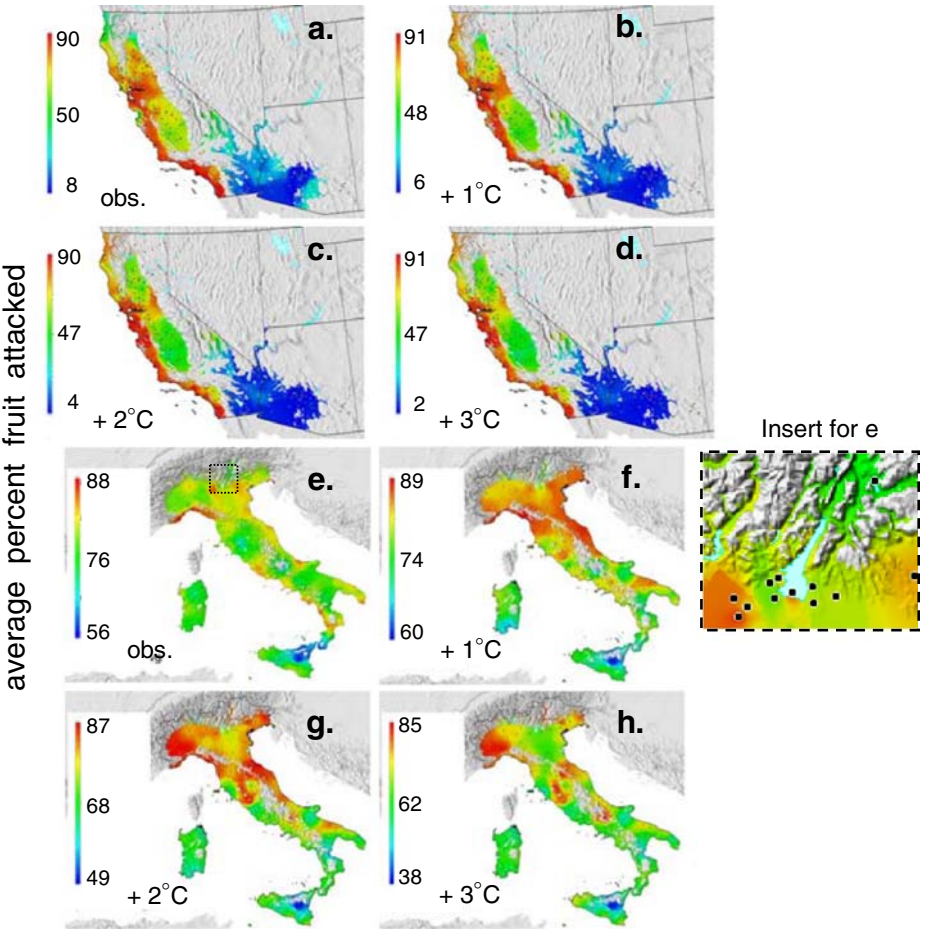

Fig. 8 Average percent olive fruit attacked in Arizona–California (**a**–**d**) and Italy (**e**–**h**) under observed and three climate-warming scenarios (+1, +2 and +3°C). The *inset* from **e** illustrates the microclimate effects around Garda Lake

fly survival and reproduction (Fig. 8c–d). High risk of fly damage will remain along the coast of California despite climate warming.

For Italy, the percentage attacked fruit using observed weather (Fig. 8e) accords well with the distribution of olive except in colder Northern areas where very low mean yield (see Fig. 6e) and low pupal densities (see Fig. 7e) were predicted, hence where low fly infestations should occur. The predicted high attack rate in northern areas may be an artifact of the use of a ratio dependent model (see Abrams 1994) with a constant search parameter ($\alpha = 0.1$, see Appendix 1) because fly search success should change with fruit densities. If F is fruit numbers and s is per capita search rate, then substituting $\alpha = (1 - \exp(-sF))$ with $s = 0.001$ yields qualitatively the correct results. Despite this deficiency, the model captures the infestations that occur around Garda Lake where the microclimate allows olive and olive fly to thrive (see inset Fig. 8e).

Higher attack rates are predicted in Italy with a 1°C increase in temperature in many areas (Fig. 8f); especially in northern Italy as weather becomes favorable for both olive (Fig. 6f) and olive fly (Fig. 7f). Increases of +2° and +3°C in temperature continue to favor olive, but cause reversals, especially in southern areas, of olive fly populations (Fig. 7g, h) and infestation levels (Fig. 8g, h) due to the negative effects of high summer temperatures on olive fly reproduction and survival.

4 Discussions

Weather is the short-run pattern of temperature, precipitation and other variables, while climate is their long run mean and variation. Climate and interacting species determines the geographic distribution of species (e.g. DeBach and Sundby 1963), but given that a species can occur in an area, weather may have a strong influence on its short term dynamics (Rochat and Gutierrez 2001). A classic study of the regional effects of weather on pest phenology and dynamics is that of the desert locust (Roffey and Popov 1968).

Anthropogenic increases in green house gases are expected to have profound effect on climate by increasing global temperatures and altering rainfall patterns (Meehl and Tebaldi 2004; Saier 2007), and this will affect all species including humans in largely unknown ways. Temperature and available moisture are two of the most important abiotic variables limiting the distribution and abundance of many species (see Andrewartha and Birch 1954), but increases in atmospheric composition (e.g. CO_2) may directly influence susceptibility of crops to pests (e.g. Hamilton et al. 2005) and may increase the severity of invasive weeds (Ziska 2003) and their tolerance to herbicides (Ziska et al. 1999). Recent investigations on climate change effects on the geographic range of pests include: arthropods (Drake 1994; Ellis et al. 1997; Fleming and Candau 1998; Williams and Liebhold 2002; Gutierrez et al. 2006, 2008a, b), and plant and animal diseases (Coakley et al. 1999; Pelley 2006).

Physiologically based models are becoming increasingly useful for separating the effects of weather (e.g. climate change) and biotic factors on species phenology and dynamics, and geographic distribution. The physiologically based growth index approach (Fitzpatrick and Nix 1968) has been widely used to determine the climatic limits and the geographic distribution of insect species (Gutierrez et al. 1974; Hughes and Maywald 1990; Sutherst et al. 1991), but this approach does not include the

dynamic or interactions of species and hence may over estimate the range (Davis et al. 1998). Tri-trophic age–mass structured physiologically based demographic models (PBDMs) can capture this biology as driven by weather, and provide a flexible tool for evaluating plant–pest interactions (Messenger and Flitters 1954). Here a PBDM of olive and olive fly was used to examine their distribution and abundance in Arizona, California, and Italy under observed weather and three climate change scenarios. The same PBDM could be used to examine their dynamics in other areas provided weather data are available.

4.1 Olive

Climate warming will alter the geographic distribution of olive bloom phenology and yield. For example, the range of olive in central California and especially in the southern reaches of AZ–CA is expected to contract. In contrast, yields are predicted to increase along north central California and along the central coast. Winter temperatures will continue to limit olive's distribution in more northern areas. In Italy, olive production is predicted to move progressively northward into previously unfavorable areas as climate warms (i.e. the Po Valley), but some contraction of favorability is predicted in hotter southern areas.

The model assumes that water availability does not affect drought tolerant olive, but this may not be the case if conditions become severe. For example, runoff from snowfall used for irrigation in California is expected to decrease (Scenarios of Climate Change in California: an Overview; http://www.energy.ca.gov/2005publications/), and increased desertification of the Mediterranean Basin is of major concern (Osborne et al. 2000; Gao and Giorgi 2008). These changes are expected to have less impact on drought tolerant species such as olive, but could have dramatic impact on less tolerant species.

4.2 Olive fly

High summer temperatures currently limit olive fly distribution in the desert areas of Arizona and south and central California, while cold limits its distribution in the far north. Climate warming is expected to further limit its abundance in many areas of California's Central Valley as summer temperature become increasingly unfavorable. In contrast, favorableness is expected to increase along the coast of California. In Italy, cold winter temperatures limit olive and the fly in northern and high elevation areas, but this is expected to change as previously unfavorable areas become favorable due to climate warming.

4.3 Concluding remarks

Geographic shifts in distribution and abundance will occur for many poikilotherm species (Gutierrez et al. 2008a). For example, pink bollworm (*Pectinophora gossypiella*) in cotton is expected to increase its current range from frost-free areas of southern California and Arizona into the cotton growing regions of Central California (Gutierrez et al. 2006). The potential geographic range of the Mediterranean fruit fly (*Ceratitis capitata*) is currently restricted to more southern climes of California where incipient populations occur (Carey 1996). Occasional

infestations occur in other unfavorable areas such as northern California (http://westernfarmpress.com/news/100107-dixon-medfly/), but winter dieback is expected to occur. However, climate warming could allow the medfly to expand its range permanently northward putting at risk major fruit growing regions of California and elsewhere. Pink bollworm and medfly are but two of a myriad of pests, weeds and diseases that could expand their range with climate warming and that need to be examined using PBDM that use daily weather. Such models are likely to give better results than models using mean weather data (Venette et al. 2000; Gutierrez et al. 2006).

A current constraint on implementing PBDMs in many cropping systems is the lack of requisite biological data for developing, refining and testing the models, and access to appropriate weather and other abiotic variables. The cost to correct this deficiency is relatively small, while the potential benefits are large. Climate models may help overcome this shortcoming as more weather variables are included and as the data become more readily available (see Hayhoe et al. 2004; Maurer 2007). The integration of improved climate models and tri-trophic PBDM*s* in a GIS would be a major step in assessing climate change effects on agricultural systems and in developing sustainable management strategies in the face of global climate change.

Acknowledgements Special thank are due the Geographic Resources Analysis Support System (GRASS) Software, ITC-irst, Trento, Italy (http://grass.itc.it) for making GIS readily available in the public domain; to Professors G. Delrio (University of Sassari, Italy), V. Girolami (University of Padova, Italy), Prof. F. Famiani (Università di Perugia, Italy), and Dr. A. Rosati (Istituto Sperimentale per l'Olivicoltura, Spoleto, Italy) for important discussions. Dr. Joyce Fox (UC/IPM) made the weather data available for California, while Professor A. Battisti (University of Padova), Dr. G. Gilioli (University of Reggio Calabria, Italy) and Mr. E. Bongioni (Provincia di Brescia, Italy) helped obtain Italian weather data for the Garda Lake region, and made weather data available.

Appendix 1: Model overview

A single plant physiologically based model for olive (Abdel-Razik 1989), and an individual based model for olive fly (Gutierrez et al. 1975, 1984, 2005; Gutierrez and Baumgärtner 1984; Gutierrez 1992, 1996; Gilioli and Cossu 2002) have been developed that proved useful in developing our model.

To analyze the effects of weather on olive and olive fly, the per capita age-structured dynamics of growth, development, reproduction, and behavior as driven by weather and their interactions was modeled incorporating the processes underpinning the biology and dynamics outlined in the text. All biological processes are driven by weather making the model is independent of time and place (i.e. physiologically based models, de Wit and Goudriaan 1978) cast in a demographic form (c.f. Gutierrez and Baumgärtner 1984; Gutierrez 1996). The details of our model are outlined here and in greater detail in Gutierrez (1996).

Physiologically based demographic models (PBDM)—common processes across trophic levels allow the same population dynamics and functional response models to be used model the number and mass dynamics and interactions of olive and olive fly (Vansickle 1977; see Di Cola et al. 1999, pp. 523–524).

Population dynamics—our model simulates the age–mass structured population dynamics of nine functional populations ($n = 1 \ldots 9$): the dynamics of olive leaf mass and numbers {models $n = 1, 2$}, stem plus shoots {$n = 3$}, root {4} and fruit mass

and number {5, 6}, olive fly in fruit {7}, and reproductive and dormant adults {8, 9}. Functions and parameters of the model are summarized in Appendix 2.

The biology of resource acquisition and allocation is embedded in a distributed maturation time demographic model used to simulate the dynamics of age–mass structured populations (1959) where time (t) and age (a) in the model are in physiological time units (text Fig. 1a; see Gutierrez 1996 and Appendix 2 for model values).

The general model for the ith age class of a population (e.g. for populations {1–6} and {8–9}) is

$$\frac{dN_i}{dt} = \frac{k\,\Delta a}{del}\left[N_{i-1}(t) - N_i(t)\right] - \mu_i(t)\,N_i(t)\,. \tag{A1}$$

N_i is the density of the ith cohort of consumer, k is the number of different age cohorts (stages), del is the expected mean developmental time, Δa is an increment in age physiological age, and $-\infty < \mu_i(t) < \infty$ is the proportional net loss rate that includes all age-species specific growth, birth, death and net immigration (see text Fig. 1b, c). The flow across all k age classes is depicted in Fig. 9a, and the pattern of emergence times for different values of Erlang parameter k are depicted in Fig. 9c. The parameter k in our model was 40. Understanding (A1) and the role $\mu_i(t)$ plays is critical to comprehending the model's construction and functioning. Computing birth and growth rates requires the use of a functional response model.

A two dimensional distributed delay model is used for olive fly larvae because the eggs are deposited in fruit of different ages that continue to develop on the plant time scale (i), while the egg–larval stage continue to develop on the fly's time scale (j). Note that net mortality of the ijth age class ($-\infty < \mu_{ij}(t) < \infty$) is also a component

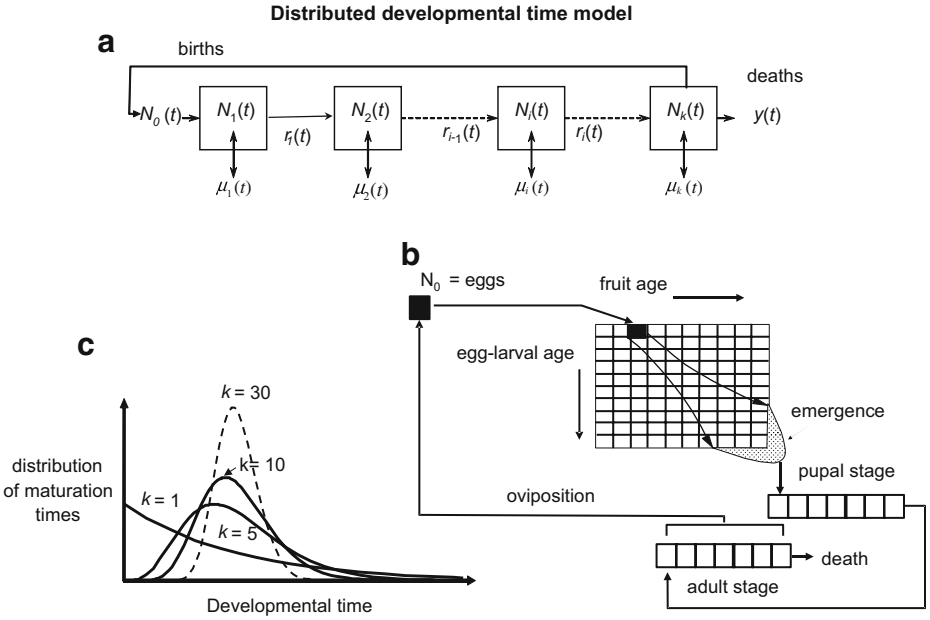

Fig. 9 (see text for explanation of figures)

of this model but is not illustrated in the figure (Fig. 9b). Note that a cohort of egg deposited on ith age fruit travel in the two dimensions.

The functional response model—a basic assumption of PBDM is that all organisms (and sub-stages) are consumers (i.e., predators in a general sense, N), and all search (α) for resources (X). The same functional response model (Eq. A2) may be used to estimate search success for all consumers for multiple resources they may seek. For example, olive leaves search for light and the roots search the soil for water and nutrients, and adult olive flies seek olive fruit to deposit their eggs.

The instantaneous per capita concave functional response model used for olive (Eq. A2) is a modified form of Watt's (1959) model (see Gutierrez 1996, p. 81), and for olive fly we use the integrated parasitoid form that allows multiple oviposition in the same fruit (i.e. the metabolic pool model; see Petrusewicz and MacFayden 1970; de Wit and Goudriaan 1978).

$$S(u) = Dh(u) = D\left[1 - \exp\left(\frac{-\alpha X}{DN}\right)\right] \tag{A2}$$

$S(u)$ is the per capita resource acquired by consumers of population N in the face of intra-specific competition (i.e. the exponent) from resource R, D is the per capita demand rate, and α is the search rate. In olive, $\alpha(N) = 1 - \exp(-sN)$ is Beer's Law of plant physiology, N is the density of leaf area (or roots) each with per capita (unit) search rate s. This makes Eq. A2 a type III functional response. For olive fly, α was assumed constant because the aggregate search behavior is not known. However, to examine discrepancies at low densities of fruit (O), $\alpha(O) = 1 - \exp(-sO)$ was used for α explaining the discrepancies (see text).

In olive, with a known set of biological state variables (mass and age structure of plant subunits) and known temperature, light, water and nutrients, the quantity of photosynthate produced $S = S(u)$ can be predicted using (A2). This production is allocated first to egestion ($1-\beta$), then respiration (i.e. Q_{10}), and after correction for conversion efficiency (λ) to reproduction and/or growth plus reserves (GR; Gutierrez and Baumgärtner 1984).

$$\mathrm{GR} = (S\beta - Q_{10})\,\lambda \tag{A3}$$

We note that S depends on D in (A2) that can be estimated under conditions of non-limiting resource by solving (A3) and assuming $D \approx S_{\max}$.

$$D \approx S_{\max} = \left(GR_{\max}(t)/\lambda + Q_{10}\right)/\beta \tag{A4}$$

D is the sum of all plant subunit demands that may vary with age, stage, sex, size, temperature and other factors, and these and consumer preferences may be included in (A2). Dividing both sides of (A2) by D yields the consumers supply–demand ratio

$$0 \le \phi_{S/D} = S/D = h(u) < 1. \tag{A5}$$

$\phi_{S/D}$ is used to scale per capita growth and fecundity from the maximum rate under optimal conditions (e.g. $\mathrm{GR} = \phi^* GR_{\max}$). The allocation is made to the subunits as

the fraction they contribute to the total demand (see Gutierrez 1996). In addition, if $O(t)$ is the number of fruit susceptible to shedding, then at any time t, the number surviving fruit equals

$$O(t+1) = O(t)\,\phi_{S/D}\,(1-\mu_O(T))\,.$$

We can model reproduction in olive fly in a similar manner. Data on olive developmental rates are summarized in Fig. 10a. Per capita reproduction at optimal temperature T^* and age x may be modeled using a beta function ($F^*(x, T^*) = ax/b^x$) where a and b are fitted constants, and $0 \le \phi_{\mathrm{OF}}(T) \le 1$ corrects for the effect of observed temperature ($F(x, T) = F^*(x, T^*)\,\phi_{\mathrm{OF}}(T)$; (see Fig. 10b; see also Fletcher and Kapatos 1983; cf. Gilioli and Cossu 2002).

The total population demand for oviposition sites by all adults $N_{\mathrm{OF}}(T)$ is

$$D_{\mathrm{OF}}(T) = \sum_{x=0}^{x_{\max}} F(x, T)\,N_{\mathrm{OF}}(x, T)\,.$$

The number of eggs (S) deposited in infested (O_{I}) and healthy fruit (O_{H}) not only depends on demand but also needs to be corrected for adult oviposition preference ($\phi_{\mathrm{pref}}(x_{\mathrm{fruit}})$, Fig. 10c) and search success. Substituting $D_{\mathrm{OF}}(T)$ and $O = \phi_{\mathrm{pref}(I)}\,O_I + \phi_{\mathrm{pref(H)}}\,O_H$ in (Eq. A2) yields total oviposition success $S(u, T) = \phi_{\mathrm{OF}}(T)\,D_{\mathrm{OF}}\,h(u, T)$ where α is the search rate. The relationship between olive fly oviposition preference and fruit growth and age are depicted in Fig. 10c where SH is the beginning of hardening of the seed.

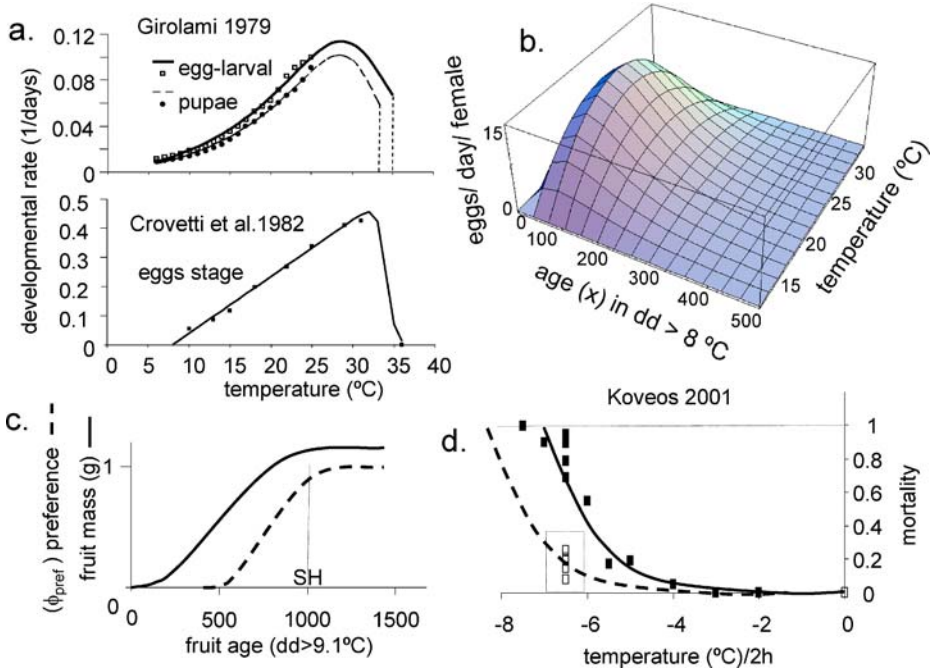

Fig. 10 (see text for explanation of figures)

The data on cold weather effects on olive fly mortality is scant, but the studies by Koveos (2001) showed that some cold hardening occurs by exposure of adult flies to cool non lethal temperature for two hours and followed by exposure to various temperatures below zero. Figure 10d summarizes all of Koveos's data with conditioning values indicated by the symbol (□) and non conditioning indicated by (■).

Appendix 2: Parameters for the olive and olive fly models

Olive subunit parameters:	
Leaf growth demand rate	$\mathrm{grl}(a) = \begin{cases} \text{if age} = a < 390, \mathrm{grl} = 0.0004\mathrm{g\ dd^{-1}} \\ \text{otherwise grl} = 0.0 \end{cases}$.
Total leaf demand	$G_{\mathrm{L}} = \sum \mathrm{grl} \times \mathrm{L}\,(a)$
Total frame demand	$G_{\mathrm{F}} := 0.5\ G_{\mathrm{L}}$
Total shoot demand	$G_{\mathrm{S}} := 1.5\ G_{\mathrm{L}}$
Total root demand	$G_{\mathrm{R}} := 0.1\ G_{\mathrm{L}}$
Total reserve demand	$G_{\mathrm{Res}} := 0.15\ G_{\mathrm{L}}$
Per capita fruit growth demand rate	$(\mathrm{grFrt}) \begin{cases} \text{if age} = a < 150, \mathrm{grFrt} = 0.00023\mathrm{g\ dd^{-1}} \\ \text{if age} = 150 < a < 1,500, \mathrm{grFrt} = 0.00082\mathrm{g\ dd^{-1}} \\ \text{otherwise grlFrt} = 0.0 \end{cases}$.
Total fruit demand	$G_{\mathrm{Frt}} = \sum \mathrm{grFrt}\,(a) \times \mathrm{Frt}\,(a)$
Leaf area	$0.1 \sum L\,(a) \cdot P\,(a)$ {$\mathrm{cm^2}$ per unit mass of leaf $L(a)$ scaled for photosynthetic efficiency with age $P(a)$}
A = area per plant	42.0 $\mathrm{m^2\ plant^{-1}}$
LAI = LA/A	
Leafing rate $\mathrm{dd^{-1}\ plant^{-1}}$	0.5 $\mathrm{dd^{-1}}$
Olive thermal threshold	9.1°C
Longevity:	
Leaves {roughly 30 months}	5,000 dd
New shoots to woody	2,500 dd
Lignified shoots	120,000 dd
Unsuberized roots	1,500 dd
Suberized roots	120,000 dd
Live frame	1,500 dd
Frame Wood	120,000 dd
Shoot wood	15,000 dd

Fruit	
Longevity to dehiscing	2,500 dd
To seed hardening	1,000 dd
To maturity	1,495 dd
Initial conditions	
Number of shoots per tree	135
Initial root mass	9,000 g
Total trunk + canes	123,000 g
Budburst delay	28.0 dd
Budburst to blooming	238 dd
Blooming to rapid growth	150 dd
Fruit rapid growth to maturity	1,495 dd
Olive fly	
Non linear developmental rate model	$\left(R(T) = aT \middle/ \left(b^{T-T_1} + c^{T_2-T}\right)\right)$
Egg–larval stages $= 0.00125T \middle/ \left(1.325^{T-37.5} + 1.0575^{2.5-T}\right)$	
Pupal stage $= 0.00105T \middle/ \left(1.5^{T-35.5} + 1.059^{3.25-T}\right)$	
Reference developmental time in degree days	
Egg	56.55 dd > 6.3°C
Larva	187 dd > 6.3°C
Pupae	248 dd > 8°C
Preoviposition	82.2 dd > 8°C
Adult	630 dd > 8°C
Dormant flies longevity	1,096 dd > 8°C
Delay parameter	k = 40
Per capita eggs female^{-1} dd^{-1}	
At age ($75 \leq a \leq 575$ dd)	$\gamma\,(a) = 0.229a \middle/ 1.0155^{a}$
Total demand for fruit per female during Δt	$0.5\phi_T \Delta t \sum_{a=75}^{575} \gamma\,(a) \times \mathrm{Fem}\,(a)$ where $\phi_T = 1.0 - \left((T - 12) - T_{\mathrm{mid}}\right) \middle/ T_{\mathrm{mid}}\Big)^2$ with T_{mid} = (34–12) / 2.0
Apparentness parameter	$\alpha = 0.1$
Critical day length for olive fly	13.4 h

References

Abdel-Razik M (1989) A model of the productivity of olive trees under optional water and nutrient supply in desert conditions. Ecol Model 45:179–204

Abrams PA (1994) The fallacies of ratio-dependent predation. Ecology 75:1842–1850

Andrewartha HG, Birch LC (1954) The distribution and abundance of animals. The University of Chicago Press, Chicago
Bigler F (1982) Post-larval mortality of the olive fly, *Dacus oleae* Gmel. (Dipt., Tephritidae) in oleaster areas of western Crete. Z Angew Entomol 93:76–89
Bigler F, Delucchi V (1981a) The main mortality factors during the prepupal development of the olive fly, *Dacus oleae* Gmel. (Dipt., Tephritidae) on oleasters and cultivated olives in Western Crete, Greece. Z Angew Entomol 92:343–363
Bigler F, Delucchi V (1981b) Evaluation of the prepupal mortality of the olive fly, *Dacus oleae* Gmel. (Dipt., Tephritidae), on oleasters and olive trees in western Crete, Greece. Z Angew Entomol 92:189–201
Bongi G (2002) Freezing avoidance in olive tree (*Olea europaea* L.): from proxies to targets of action. Adv Hort Sci 16:117–124
Carey JR (1996) The incipient Mediterranean fruit fly population in California: implications for invasion biology. Ecology 77:1690–1697
Coakley S, Scherm H, Chakraborty S (1999) Climate change and plant disease management. Annu Rev Phytopathol 37:399–426
Crovetti A, Loi G, Quaglia F, Belcari A (1981) Influence of constant temperature on embryonic development of olive-fruit fly (*Dacus oleae* Gmel.). Frustula Entomol 17:83–91
Crovetti A, Quaglia F, Loi G, Rossi E, Malfatti P, Chesi F, Conti B, Belcari A, Raspi A, Paparatti B (1982) Influence of temperature and humidity on the development of the immature stages of *Dacus oleae* (Gmelin). Frustula Entomol 5:133–166
Davis AJ, Jenkinson LS, Lawton JH, Shorrocks B, Wood S (1998) Making mistakes when predicting shifts in species range in response to global warming. Nature 391:783–786
DeBach P, Sundby RA (1963) Competitive displacement between ecological homologues. Hilgardia 34:105–166
De Melo-Abreu JP, Barranco D, Cordeiro AM, Tous J, Rogado BM, Villalobos FJ (2004) Modelling olive flowering date using chilling for dormancy release and thermal time. Agric For Meteorol 125:117–127
de Wit CT, Goudriaan J (1978) Simulation of ecological processes. PUDOC, The Netherlands
Delrio G, Prota R (1988) Determinants of abundance in a population of the olive fruit-fly. Frustula Entomol 11:47–55
Denney JO, McEachern GR, Griffiths JF (1985) Modeling the thermal adaptability of the olive (*Olea europaea* L.) in Texas. Agric For Meteorol 35:309
Di Cola G, Gilioli G, Baumgärtner J (1999) Mathematical models for age-structured population dynamics. In: Huffaker CB, Gutierrez AP (eds) Ecological entomology. Wiley, New York
Drake VA (1994) The influence of weather and climate on agriculturally important insects: an Australian perspective. Aust J Agric Res 45:487–509
Ellis WN, Donner JH, Kuchlein JH (1997) Recent shifts in phenology of Microlepidoptera, related to climatic change (Lepidoptera). Entomol Berichten (Amsterdam) 57:66–72
Fiorino P (ed) (2003) Olea: Trattato di olivicoltura. Edagricole, Bologna
Fitzpatrick EA, Nix HA (1968) The climatic factor in Australian grasslands ecology. In: Moore RM (ed) Australian grasslands. Australian National University Press
Fleming RA, Candau J-N (1998) Influences of climatic change on some ecological processes of an insect outbreak system in Canada's boreal forests and the implications for biodiversity. Environ Monit Assess 49:235–249
Fletcher BS, Kapatos ET (1983) An evaluation of different temperature-development rate models for predicting the phenology of the olive fly *Dacus oleae*. Fruit flies of economic importance Proceedings of the CEC/IOBC International Symposium, Athens, Greece, 16 19 November 1982. 1983; 321 329, Rotterdam Netherlands: A.A. Balkema
Fletcher BS, Pappas S, Kapatos E (1978) Changes in the ovaries of olive flies (*Dacus oleae* (Gmelin)) during the summer, and their relationship to temperature, humidity and fruit availability. Ecol Entomol 3:99–107
Gao X, Giorgi F (2008) Increased aridity in the Mediterranean region under greenhouse gas forcing estimated from high resolution simulations with a regional climate model. Glob Planet Change 62:195–209
Genç H, Nation JL (2008) Survival and development of Bactrocera oleae Gmelin (Diptera: Tephritidae) immature stages at four temperatures in the laboratory. Afr J Biotechnol 7:2495–2500
Gilioli G, Cossu A (2002) First validation of an individual-based model for the population dynamics of *Bactrocera oleae* (Gmelin). Atti XIX Congresso Nazionale di Entomologia, Catania, 10–15 giugno 34–39

Girolami V (1979) Studies on the biology and population ecology of *Dacus oleae* (Gmelin). 1. Influence of environmental abiotic factors on the adult and on the immature stages. Redia 62:147–191

Gutierrez AP (1992) The physiological basis of ratio dependent theory. Ecology 73:1552–1563

Gutierrez AP (1996) Applied population ecology: a supply–demand approach. Wiley, New York, USA

Gutierrez AP, Baumgärtner JU (1984) Multitrophic level models of predator–prey energetics: I. Age-specific energetics models—pea aphid *Acyrthosiphon pisum* (Homoptera: Aphididae) as an example. Can Entomol 116:924–932

Gutierrez AP, Havenstein DE, Nix HA, Moore PA (1974) The ecology of *Aphis craccivora* Koch and Subterranean Clover Stunt Virus in south-east Australia. II. A model of cowpea aphid populations in temperate pastures. J Appl Ecol 11:1–20

Gutierrez AP, Falcon LA, Loew W, Leipzig PA, van-den Bosch R (1975) An analysis of cotton production in California: a model for acala cotton and the effects of defoliators on its yields. Environ Entomol 4:125–136

Gutierrez AP, Baumgärtner JU, Summers CG (1984) Multitrophic level models of predator–prey energetics: III. A case study of an alfalfa ecosystem. Can Entomol 116:950–963

Gutierrez AP, Pitcairn MJ, Ellis CK, Carruthers N, Ghezelbash R (2005) Evaluating biological control of yellow starthistle (*Centaurea solstitialis*) in California: a GIS based supply–demand demographic model. Biol Control 34:115

Gutierrez AP, d'Oultremont T, Ellis CK, Ponti L (2006) Climatic limits of pink bollworm in Arizona and California: effects of climate warming. Acta Oecol 30:353–364

Gutierrez AP, Ponti L, d'Oultremont T, Ellis CK (2008a) Climate change effects on poikilotherm tritrophic interactions. Clim Change 87:S167–S192

Gutierrez AP, Daane KM, Ponti L, Walton VM, Ellis CK (2008b) Prospective evaluation of the biological control of vine mealybug: refuge effects and climate. J Appl Ecol 45:524–536

Hamilton JG, Dermody O, Aldea M, Zangerl AR, Rogers A, Berenbaum MR, Delucia EH (2005) Anthropogenic changes in tropospheric composition increase susceptibility of soybean to insect herbivory. Environ Entomol 34:479–455

Hartmann HT, Opitz KW (1980) Olive production in California. Leaflet 2474 University of California Div. Agric. Sci., Davis, USA

Hayhoe K, Cayan D, Field C, Frumhoff P, Maurer E, Miller N, Moser S, Schneider S, Cahill K, Cleland E, Dale L, Drapek R, Hanemann RM, Kalkstein L, Lenihan J, Lunch C, Neilson R, Sheridan S, Verville J (2004) Emissions pathways, climate change, and impacts on California. Proc Natl Acad Sci USA 101:12422–12427

Hughes RD, Maywald GW (1990) Forecasting the favorableness of the Australian environment for the Russian wheat aphid, *Diuraphis noxia* (Homoptera: Aphididae), and its potential impact on Australian wheat yields. Bull Entomol Res 80:165–175

Kapatos ET, Fletcher BS (1984) The phenology of the olive fly, *Dacus oleae* (Gmel.) (Diptera, Tephritidae), in Corfu. Z Angew Entomol 97:360–370

Kapatos ET, Fletcher BS (1986) Mortality factors and life-budgets for immature stages of the olive fly, *Dacus oleae* (Gmel.) (Diptera, Tephritidae), in Corfu. J Appl Entomol 102:326–342

Koveos DS (2001) Rapid cold hardening in the olive fruit fly *Bactrocera oleae* under laboratory and field conditions. Entomol Exp et Appl 101:257–263

Koveos DS, Tzanakakis ME (1990) Effect of the presence of olive fruit on ovarian maturation in the olive fruit fly, *Dacus oleae*, under laboratory conditions. Entomol Exp et Appl 55:161

Mancuso S, Pasquali G, Fiorino P (2002) Phenology modelling and forecasting in olive (*Olea europaea* L.) using artificial neural networks. Adv Hort Sci 16:155–164

Maurer EP (2007) Uncertainty in hydrologic impacts of climate change in the Sierra Nevada, California, under two emissions scenarios. Clim Change 82:309–325

Meehl GA, Tebaldi C (2004) More intense, more frequent, and longer lasting heat waves in the 21st century. Science 305(5686):994–997

Messenger PS, Flitters NE (1954) Bioclimatic studies of three species of fruit flies in Hawaii. J Econ Entomol 47:756–765

Mita L, Mitasova H (2002) Spatial interpolation. University of Illinois at Urban-Champaign, Urbana, IL

Orlandi F, Fornaciari M, Romano B (2002) The use of phenological data to calculate chilling units in *Olea europaea* L. in relation to the onset of reproduction. Int J Biometeorol 46:2–8

Osborne CP, Chuine I, Viner D, Woodward FI (2000) Olive phenology as a sensitive indicator of future climatic warming in the Mediterranean. Plant, Cell & Environ 23:701–710

Palese AM, Celano G, Xiloyannis C (2000) Le esigenze nutrizionali dell'olivo. Frutticoltura 62:50–53
Pelley J (2006) Perspective: will global climate change worsen infectious diseases? Environ Sci & Tech 40:2502–2503
Petrusewicz K, MacFayden A (1970) Productivity of terrestrial animals: principles and methods. Blackwell, Oxford
Proietti P, Tombesi A, Boco M (1994) Influence of leaf shading and defoliation on oil synthesis and growth of olive fruits. Acta Hort 356:272–277
Pucci C, Forcina A, Salmistraro (1981) Effects of temperature on the death rate of larvae, pupation and activities of parasites for *Dacus oleae* (Gmel.). Frustula Entomol 17:143–155
Ricci C, Ambrosi G (1981) The oviposition by *Dacus oleae* (Gmel.) and the size of the olives. Frustula Entomol 17:181–195
Rice RE, Phillips PA, Stewart-Leslie J, Sibbett GS (2003) Olive fruit fly populations measured in Central and Southern California. Calif Agric 57:122–127
Rochat J, Gutierrez AP (2001) Weather-mediated regulation of olive scale by two parasitoids. J Anim Ecol 70:476–490
Roffey J, Popov G (1968) Environmental and behavioural processes in Desert locust outbreaks. Nature 219:446–450
Saier MHJ (2007) Climate change, 2007. Water Air Soil Pollut 181:1–2
Sanz-Cortés F, Martínez-Calvo J, Badenes ML, Bleiholder H, Hack H, Llácer G, Meier U (2002) Phenological growth stages of olive trees (*Olea europaea*). Ann Appl Biol 140:151–157
Sutherst RW, Maywald GF, Bottomly W (1991) From CLIMEX to PESKY, a generic expert system for risk assessment. EPPO Bulletin 21:595–608
Tzanakakis ME, Koveos DS (1986) Inhibition of ovarian maturation in the olive fruit fly, *Dacus oleae* (Diptera: Tephritidae), under long photophase and an increase of temperature. Ann Entomol Soc of Amer 79:15–18
Vansickle J (1977) Attrition in distributed delay models. IEEE T Syst Man Cyb 7:635–638
Venette RC, Naranjo SE, Hutchison WD (2000) Implications of larval mortality at low temperatures and high soil moistures for establishment of pink bollworm (Lepidoptera: Gelechiidae) in Southeastern United States cotton. Environ Entomol 29:1018–1026
Vitagliano C, Sebastiani L (2002) Physiological and biochemical remarks on environmental stress in olive (*Olea europaea* L.). Acta Hort 586:435–440
Watt KEF (1959) A mathematical model for the effects of densities of attacked and attacking species on the number attacked. Can Entomol 91:129–144
Williams DW, Liebhold AM (2002) Climate change and the outbreak ranges of two North American bark beetles. Agric Forest Entomol 4:87–99
Zambetaki A, Mavragani-Tsipidou P, Scouras ZG (2000) Heat shock response of *Bactrocera oleae* (Diptera: Tephritidae): genes and proteins. Ann Entomol Soc Amer 93:648–652
Zangheri S, Cavalloro R, Delrio G, Girolami V, Prota R, Ricci C (1976) Observations on *Dacus oleae* Gmelin in various regions of Italy, within the context of a coordinated programme. Atti XI Congresso Nazionale Italiano di Entomologia, Pauda, Italy, pp 429–436
Ziska LH (2003) Evaluation of growth response of six invasive species to past, present, and future atmospheric CO_2. J Exp Bot 54:395–406
Ziska LH, Teasdale JR, Bunce JA (1999) Future atmospheric CO_2 may increase tolerance to glyphosate. Weed Sci 47:608–615